

Mud-crack pattern evolution in iterated drying cycles

Mary Miedema

Department of Physics, University of Toronto

(Dated: May 13, 2015)

This experiment examined pattern formation in crack networks of montmorillonite clay over a series of wetting and drying cycles. The evolution of a mud-crack pattern approximately 6.5 mm thick was analyzed for forty-five cracking cycles. Over each iteration, as the mud-cracks closed and re-cracked roughly along their previous positions, a clear evolution from 90° - 90° - 180° T-junctions to 120° - 120° - 120° Y-junctions was observed. However, pockets of air trapped in the mud during the wetting process caused this evolution to be incomplete and acted as a limiting factor in the experiment.

I. INTRODUCTION AND THEORY

Fracture networks are ubiquitous in nature, and mud-cracks are among the most common of fracture networks. The highly dynamic nature of cracking processes makes the propagation of cracks a very suitable candidate for pattern formation. Recent experiments have examined many of these pattern formation processes, from crack patterns in the presence of electromagnetic fields [1, 2] to the effects of external vibrations and flow patterns on crack propagation [3]. It is nature itself, however, which provides one of the most striking examples of pattern formation in mud-crack networks.

Fig. 1 shows several naturally occurring crack patterns; in particular, panels B) and C) depict examples of a distinctive hexagonal crack pattern. This pattern is thought to have evolved through a series of wetting and drying cycles (or in the case of Antarctic permafrost, annual freezing and thawing cycles)[4].

Goehring *et al.* attempted to experimentally reproduce this process of pattern evolution by observing crack networks formed in a thin layer of bentonite clay during 25 wetting and drying cycles [5]. In this experiment, vertices were observed to evolve from 90° - 90° - 180° T-junctions to 120° - 120° - 120° Y-junctions with a relaxation time of approximately four cracking iterations. Goehring *et al.* put forward a simple model of crack behaviour to explain this behaviour, based on Irwin's theory of fracture.

Irwin examined fracture mechanics in the context of stress, specifically identifying the way in which stress concentrates around the tip of a crack (or other defect) [6]. This concentration of stress means that as a crack propagates, it largely relieves stress perpendicular to its sides. So, if a second crack approaches the first, it turns to meet the first crack at a right angle in order to relieve the most remaining stress energy [7]. This results in the formation of 90° - 90° - 180° vertex angles known as T-junctions.

Goehring *et al.* proposed that as a mud-crack pattern is wet so as just to close its cracks, and then allowed to dry and re-crack, the new cracks will form along the old crack network, as these are lines of weakness for the mud [5]. However, the sequence in which cracks meet at vertices may change randomly with each cracking cycle. For this reason, a symmetric 120° Y-junctions will slowly



FIG. 1. A range of naturally occurring crack patterns: A) shows a rectilinear pattern in dried creek beds (image ©Alan Parkinson and licensed for reuse under a Creative Commons License); B) shows a hexagonal pattern in Death Valley, CA (image ©Lauri Väin and licensed for reuse under a Creative Commons License); C) shows polygonal terrain in Antarctic permafrost (image courtesy of Lucas Goehring). Panel D) shows a sample of the montmorillonite crack patterns produced in this experiment.

emerge. This process is illustrated in Fig. 2.

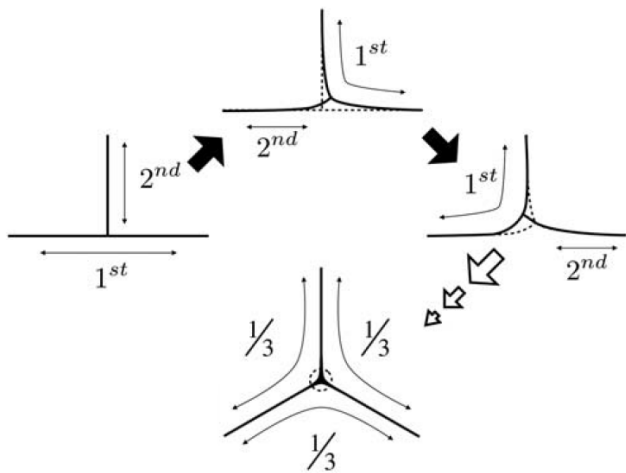


FIG. 2. As the sequence in which a vertex cracks is randomly decided in each wetting/drying cycle, the vertex evolves from a T-junction to a Y-junction. For instance, in the second iteration, the first crack may approach the vertex from what was formerly the secondary crack, and will thus curve left or right. The second crack will once again approach the first crack at a right angle. The position of the vertex itself moves slightly to accommodate this change. Over many iterations, this random process will result in the formation of a symmetric vertex. Image from [5]

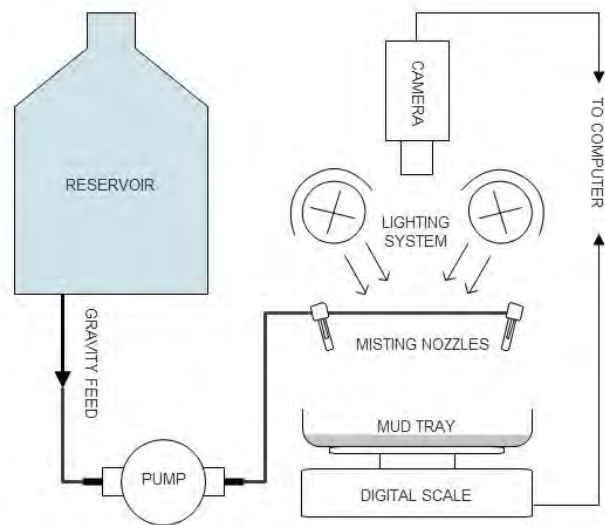


FIG. 3. Depicted is the system used to monitor and re-wet mud samples. A digital camera was used to track crack patterns in the mud at intervals of two minutes.

This experiment attempted to test this model for mud-crack pattern evolution over a longer series of crack cycles, and in a more controlled environment, than Goehring *et al.*'s original experiment.

II. APPARATUS AND EXPERIMENT

This experiment was designed to be more automated and rigorously controlled than that of Goehring *et al.*, who used a spray bottle by hand to wet a series of mud samples [5]. To this end, a 15.0 by 20.5 cm polystyrene tray of mud was placed on a digital scale so that its weight could be measured continuously. The mud was wet by four misting nozzles placed approx. 30 cm above the tray, which were controlled by a small pump (operating at 150 psi). The pump was supplied via gravity feed from a reservoir of distilled water. Above the misting nozzles was a fluorescent lighting system, which served to gently warm the tray and facilitate faster drying, as well as a camera system to monitor the experiment. Fig. 3 shows a schematic diagram of the experiment.

Each mud sample was initially prepared by mixing montmorillonite clay (Acros Organics, Montmorillonite K-10) and distilled water in a 1:1 weight ratio. Over the course of over twenty runs, a range of sample sizes were tested. The most successful and longest run contained 80.0 ± 0.2 g of montmorillonite, with a sample thickness of 6.5 ± 0.2 mm. The number of cycles which could be observed for a given run was limited by the formation of air bubbles in the mud. The effect of this trapped air on the sample will be discussed later in this paper. Thicker mud samples proved more resilient to this bubbling process, but since the spacing of desiccation cracks increases with the thickness of the cracking layer [5], there was a trade-off in sample size in return for this increased longevity. For the longest run, forty-five cycles were observed over a period of two weeks (each wetting and drying iteration took approx. eight hours).

For each run, Labview was used to monitor the weight and drying rate of the mud sample, turning on the pump when a threshold drying rate of -0.002 g/s had been reached. This threshold rate was chosen so that all cracks would have ample time to open before re-wetting. The pump would then run for a set period of time to re-wet the tray, until the sample reached just over twice its dry weight, which was sufficient to close the mud-crack network.

III. ANALYSIS

By tracking the position of several calibration markers in a series of images, the measurement error for the camera system was determined to be at most one or two pixels. In comparison, statistical error due to sample size played a far more significant role during image analysis.

For each run, the image taken immediately prior to the subsequent wetting/drying cycle was processed using MATLAB. MATLAB's *edge()* function combined with the *canny* method examined the image's gradient to extract the position of cracks in the original image. A number of noise processing functions were applied to clean the crack network, removing flaws in the surface of the mud

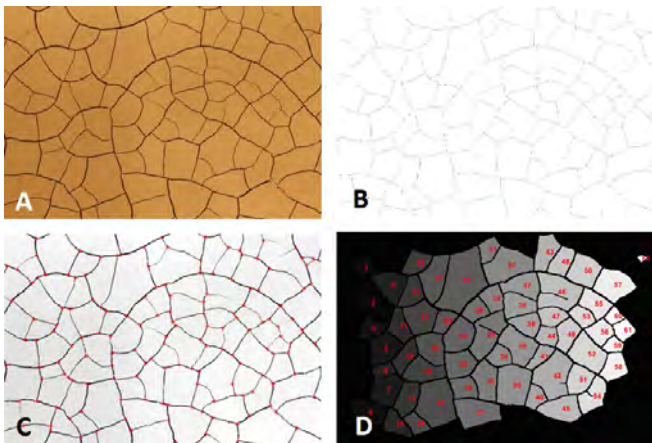


FIG. 4. Image processing: A) gives the original image, B) shows the skeleton image, C) shows the threshold image with positions of vertices indicated in red, and D) shows the image with each ped labelled by a different pixel value to determine area (the border peds were disregarded).

and creating a threshold image. The *bwlabel()* function was used to label each ped with a different pixel value, which could then be counted to determine area statistics.

A series of dilations, erosions, and skeletonizations through the *bwmorph()* function were further applied to the threshold image to create a skeleton image, that is, a single pixel outline of the crack network. The locations of branchpoints, where the network crossed itself, were extracted also using *bwmorph()*; and the identification of independent vertices was ensured using the *pdist()* and *squareform()* functions to remove any branchpoints which were too close to each other. Fig. 4 demonstrates these stages of image processing.

Using the skeleton image and the location of these vertices, for each iteration both the position of each vertex and its angles could be obtained. For each image, the nearest neighbour of each vertex from the previous iteration was found using *knnsearch()*. The displacement of this vertex could then be obtained (and if over a certain threshold, would be discarded to ensure that formation of new vertices would not contribute). The process by which vertex angles were found is described in Fig. 5.

IV. RESULTS AND DISCUSSION

Qualitatively, as shown in Fig. 6, the crack pattern mostly cracked along its previous position, as expected. However, in later runs the network tended to diverge more significantly from its former pattern; the formation of unrelated crack patterns seemed closely correlated to the presence of air bubbles trapped within the sample. Despite this, an overall progression from a rectilinear to a more generally polygonal network is apparent.

Fig. 7 displays the vertex angle distribution for the sample over time, as well as its standard deviation. It

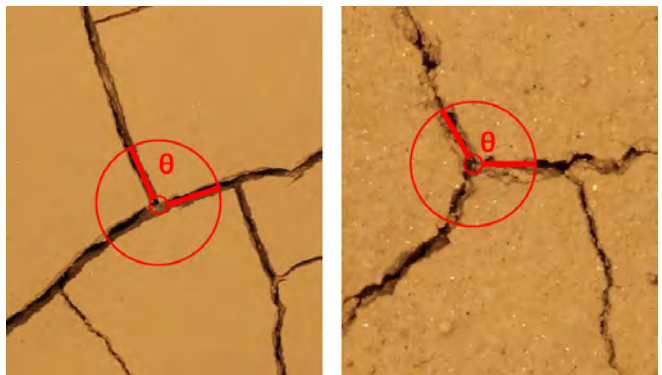


FIG. 5. Vertex angles were determined by drawing two circles around each vertex, then finding the positions at which each crack intersected these circles. Each crack was then approximated by a line, and the phase angle of this line was found using MATLAB's *angle()* function. The difference between phase angles gave the desired three vertex angles. The above image shows this process performed for the same vertex, for both its first and eighth iteration. The vertex clearly begins as a T-junction, but by its eighth cracking cycle has evolved into a Y-junction. The position of the vertex itself has shifted slightly to accommodate this change. A video version of this figure may be found [here](#) or [here](#)

is clear that initially the crack pattern is dominated by T-junctions, as evidenced by the large peaks near 90° and just below 180° . Over the first ten cycles, the angle distribution becomes centered at 120° , indicating an increasing number of Y-junctions, and slowly approaches a more Gaussian form. Over the next thirty-five cycles, the angle distribution remains essentially the same. Similar results were observed by Goehring *et al.*, although their angle distribution underwent evolution in the first five iterations, which is reasonable considering that their mud sample was only 2.9 ± 0.1 mm thick.

As previously mentioned, a significant problem was the formation of air pockets in the mud sample as air was incorporated into the sample along with the fine mist used for wetting. As per Irwin's theory of fracture, stress concentrates around defects in the cracking medium, so these air bubbles acted as sites for crack formation. So, while most cracks formed along the previous crack pattern, some new cracks formed around air pockets. These new cracks formed T-junctions in each iteration, instead of evolving towards Y-junctions. This resulted in a large spread in the angle distribution, even after many iterations. One might have expected, in the absence of air pockets, a narrower peak around 120° , although this process is too random and complex to ever fully converge to 120° .

So, while Goehring *et al.* found that their standard deviation reached a constant value after a rapid decrease in the first ten iterations [5], the wide spread of angles introduced to this experiment by bubbling caused the standard deviation of vertex angles to remain essentially constant.

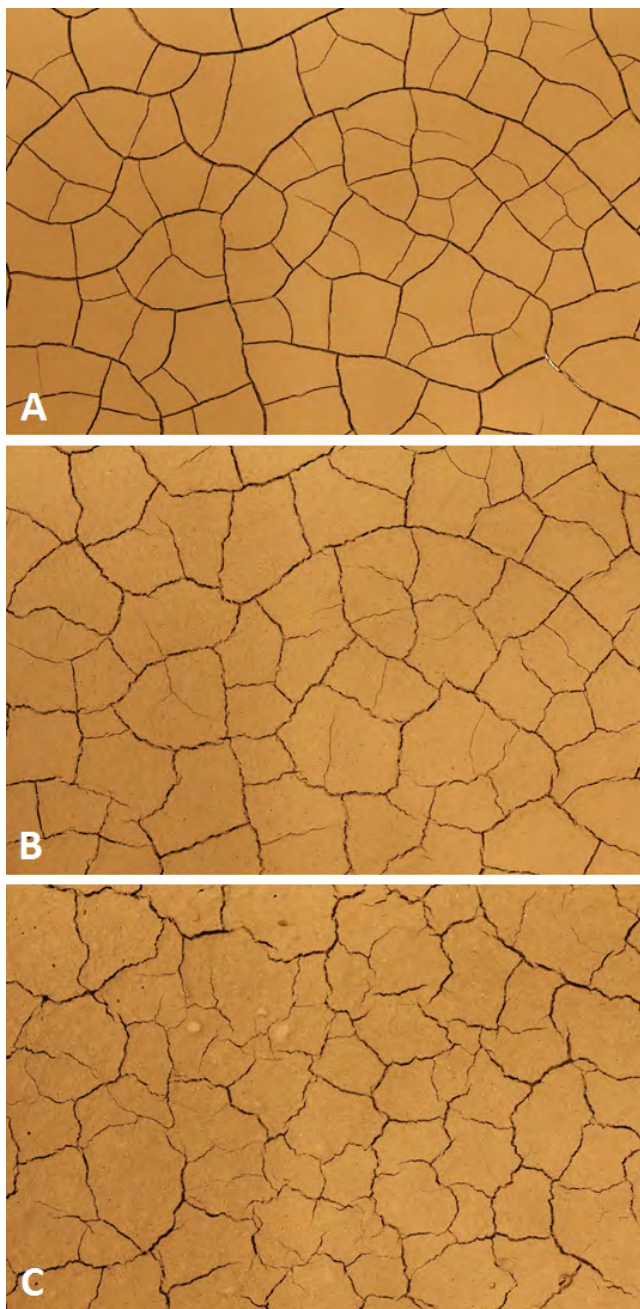


FIG. 6. The crack network imaged during its first (A), eighth (B), and forty-fifth (C) iterations. The disfiguration caused by bubbles is clear in the centre of C). A video version of this figure may be found [here](#) or [here](#) .

The number of neighbours for each ped was counted for the first twenty iterations (after this the lack of fully delineated peds made the assignment of neighbours too arbitrary). Bohn *et al.* analyzed crack patterns and showed that the average number of neighbours for any ped should be six, if all vertices are formed by three cracks [7]. Thus, as plotted in Fig. 8, the number of neighbours should be a distribution centred at six. In this case, the distribution moves from double peaks at 5 and 7 to a more

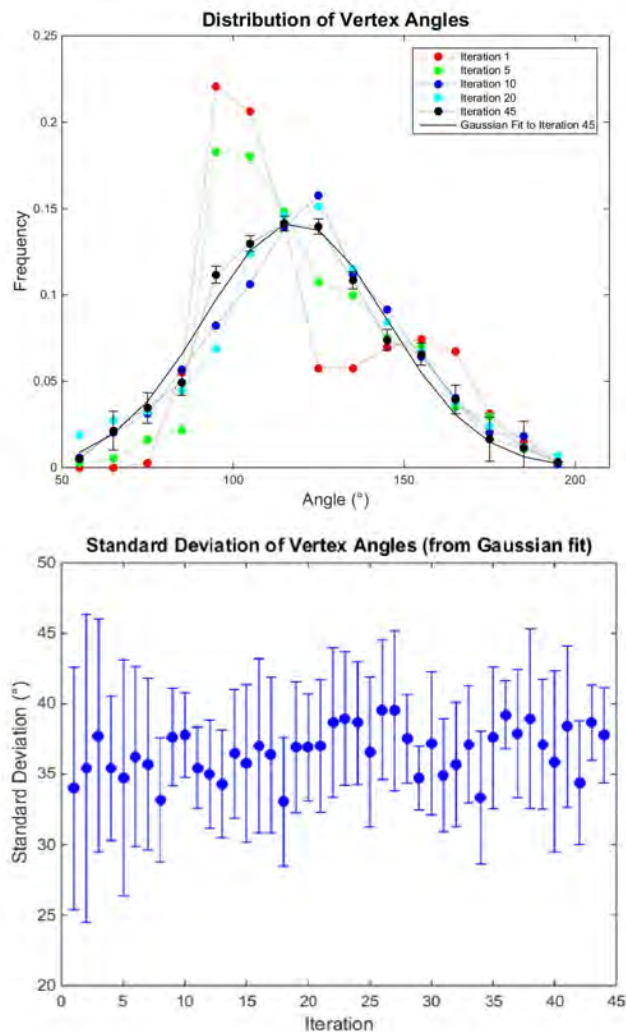


FIG. 7. Above: vertex angle distribution for several iterations; the forty-fifth iteration is fitted to a Gaussian for comparison. Representative error bars are plotted for the final iteration. Below: standard deviation of angle distributions obtained from Gaussian fitting for each iteration.

central peak at 6, indicating a general shift to a hexagonal pattern. However, this shift was again curtailed by the formation of bubbles, which tended to result in a more open crack pattern without clearly defined peds (cf. Fig. 6).

The lack of ped definition caused similar problems for area measurements (Fig. 9), although the actual distribution of areas did not appear to change significantly during the cracking cycles.

Displacement was tracked for each vertex and averaged for each iteration; the results are given in Fig. 10. Vertex displacement from the original vertex position (in the original crack network) sharply increases during the first twenty cracking cycles, but then plateaus. Goehring *et al.*'s experiment suggested that this displacement continuously increases as vertices weakly tend to move along

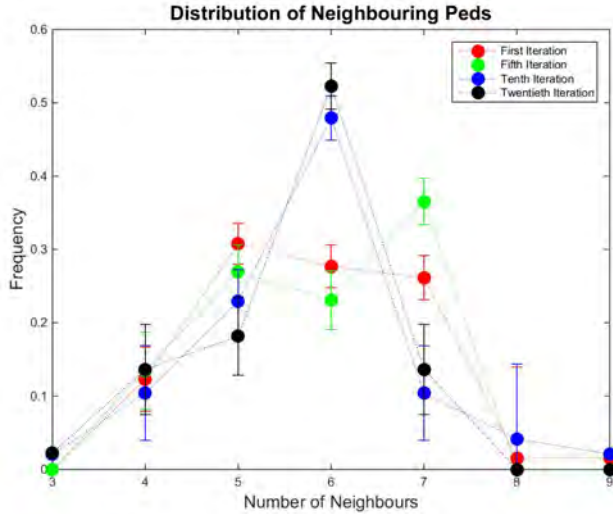


FIG. 8. Distribution of the number of neighbouring peds counted for several iterations.

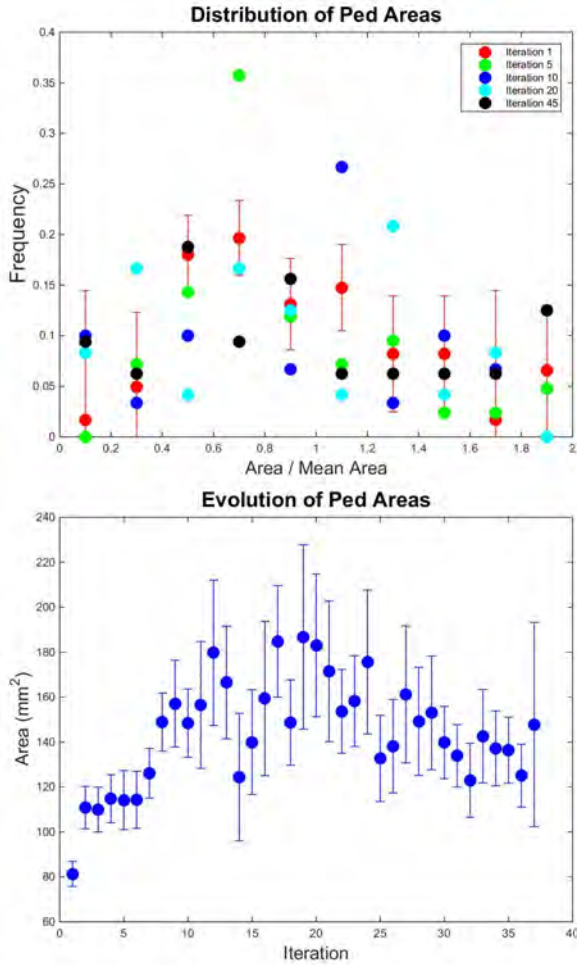


FIG. 9. Above: area distribution for several iterations. Representative error bars are shown for the first iteration. Below: mean area of peds vs. cracking iterations.

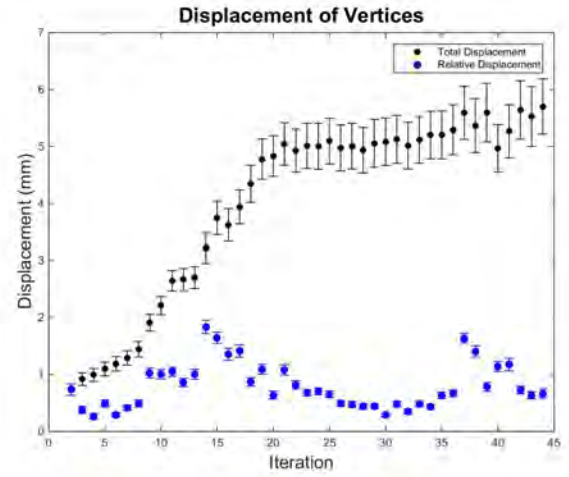


FIG. 10. Vertex displacement: in blue is the average displacement of vertices from the previous iteration; in black is the average total displacement of vertices from the original crack network.

the original network's secondary cracks [5]. However, it is more reasonable to think that this displacement eventually tapers off as the influence of the original network lessens and the sequence of crack formation becomes more random, which agrees with the results of this experiment. Interestingly, the instances of greater relative vertex displacement (plotted in blue) seem to correspond to very slightly wetter iterations. This suggests that control of the wetting process may need to be tightened so as to account for humidity and other minor fluctuations in misting procedures in future versions of this experiment.

V. CONCLUSIONS

This experiment examined mud-crack pattern evolution in montmorillonite clay over a series of wetting and drying cycles. The evolution of a crack network approximately 6.5 mm thick was analyzed over forty-five cracking cycles. As the mud-cracks closed and re-cracked along their previous positions, a clear evolution from 90° - 90° - 180° T-junctions to 120° - 120° - 120° Y-junctions was observed. However, small bubbles of air which were trapped in the mud during the wetting process interfered with the re-opening of cracks along their previous positions and instead caused the formation of entirely new cracks. This was problematic both because it decreased the overall longevity of mud samples and because it reduced the proportion of mud-cracks evolving towards Y-junctions during the wetting/drying process. Future experiments wishing to examine the behaviour of mud-cracks over a longer series of cracking cycles will have to address this problem, which could be mitigated by increasing the scale of the experiment or protecting the mud sample from air during wetting. Despite this limiting factor of air pockets, however, the mud sample proved surprisingly robust

in its overall evolution from T-junctions to Y-junctions.

knowledges the advice of Lucas Goehring regarding image analysis.

VI. ACKNOWLEDGEMENTS

The author would like to thank the supervising professor, Stephen Morris. The author also gratefully ac-

-
- [1] T. Khatun, M. Choudhury, T. Dutta, and S. Tarafdar, Phys. Rev. E **86**, 016114 (2012).
 - [2] L. Pauchard, F. Elias, P. Boltenhagen, A. Cebers, and J. Bacri, Phys. Rev. E **77**, 021402 (2008).
 - [3] A. Nakahara and Y. Matsuo, Phys. Rev. E **74**, 045102(R) (2006).
 - [4] L. Goehring and S. W. Morris, Phys. Today **67**, 39 (2014).
 - [5] L. Goehring, R. Conroy, A. Akhter, W. J. Clegg, and A. F. Routh, Soft Matter **6**, 35623567 (2010).
 - [6] L. Goehring, A. Nakahara, T. Dutta, S. Kitsunzaki, and S. Tarafdar, *Desiccation Cracks and their Patterns: Formation and Modelling in Science and Nature* (Wiley, 2015).
 - [7] S. Bohn, L. Pauchard, and Y. Couder, Phys. Rev. E **71**, 046214 (2005).